Volume 70 • Issue 2 • June 2015

Journal of Achievements in Materials and Manufacturing Engineering

International Scientific Journal published monthly by the World Academy of Materials and Manufacturing Engineering

The corrosion performance of Zn-Al-Mg based alloys with tin addition in neutral salt spray environment

J. Gondek, M. Babinec, M. Kusý*

Institute of Materials Science, Faculty of Material Science and Technology, Slovak University of Technology, Paulínska 16, 917 24 Trnava, Slovakia

* Corresponding e-mail address: martin.kusy@stuba.sk

ABSTRACT

Purpose: Ternary Zn-Al-Mg system was modified with 0.5, 1.0, 2.0 and 3.0 wt. % of Sn in order to study its microstructure, phase composition and corrosion performance in neutral salt spray test. Addition of tin was devised to modify phase composition and phase quantities, particularly Zn_2Mg intermetallic phase.

Design/methodology/approach: Ternary and quaternary alloys were prepared from 4N purity elements under a flux layer. Chemical composition was verified using optical emission spectrometer. Light and scanning electron microscopy was used to study microstructure further complemented with local chemical analysis using energy dispersive X-ray spectrometry. Phase composition and phase quantity of as-cast samples and samples after corrosion tests were determined using X-ray diffraction. Performance of alloys in neutral salt spray test was evaluated by method of weight change.

Findings: Addition of Sn caused change in solidification mechanism which influenced also phase composition and phase quantity. Typical weight loss was determined after exposure of ternary system in salt spray chamber. Contrary, weight gain was observed in all four tin alloyed ternary systems. This finding was explained by blister formation.

Research limitations/implications: Results introduced in this paper are limited to relatively slowly cooled coarse-grained samples. Different cooling rates may affect phase composition and also corrosion performance.

Practical implications: Paper shows alternative way of changing phase composition of ternary Zn-Al-Mg system by alloying using tin. Change in phase composition may have, however, impact on corrosion performance as it is shown in this paper.

Originality/value: Paper describes change of the corrosion mechanism when ternary Zn-Al-Mg system is alloyed with Sn. It also shows that blister formation found in quaternary system depends on grain orientation with respect to the exposed surface.

Keywords: Corrosion; Zn-based alloy; Zn-Al-Mg alloy; Microstructure analysis; blistering

Reference to this paper should be given in the following way:

J. Gondek, M. Babinec, M. Kusý, The corrosion performance of Zn-Al-Mg based alloys with tin addition in neutral salt spray environment, Journal of Achievements in Materials and Manufacturing Engineering 70/2 (2015) 70-77.

PROPERTIES

1. Introduction

In general, zinc based coatings corrodes about 100 times slower in comparison with steel for cold forming [1]. Zn-Al-Mg system (ZAM) brings next improvement in corrosion resistance. This zinc based coatings with additions of aluminium and magnesium were developed in 1990s and during the last decade have developed significantly [2,3]. ZAM coatings are characteristic by markedly higher corrosion resistance in high chloride environment in comparison with conventional hot dip galvanized steel [2]. Reasons for better corrosion resistance of ZAM coatings is not yet satisfactory explained. Literature offers a variety of results of corrosion tests; however proposed explanations are often different [4]. Corrosive process of zinc based coatings is often explained by dissolving-precipitating mechanism. By this mechanism, Zn^{2+} ions are released as anodic part and hydroxide ions are formed as cathodic part of reaction due to reduction of oxygen. These ions (Zn^{2+}, OH^- and their combinations with other ions present in electrolyte) can precipitate generating various corrosion products. Adding aluminium and magnesium into pure zinc caused a formation of new oxide layers and complex corrosion products after corrosion tests. These were not present in case of pure zinc coatings [1]. Higher corrosion resistance used to be attributed to presence of these new corrosion products, especially aluminium oxides and zinc-aluminium hydroxides with general formula $Zn_xAl_y(A)_m(OH)_n{\cdot}zH_2O$ (*A* represents anion, usually carbonate in case of atmospheric corrosion) [2]. Magnesium addition to binary Zn-Al alloy results in formation of intermetallic phases most often with zinc, usually Zn_2Mg or $Zn_{11}Mg_2$. Zn-Mg based intermetallic compounds are more corrosion active than a pure zinc and therefore they corrode predominately. Binary and ternary eutectics are also detected in ZAM coatings. It is commonly known that these are more corrosion susceptible than pure zinc. Literature offers three hypothesis of corrosion behavior of ZAM coatings. Dissolution of intermetallic phases plays a center role in formation of Mg^{2+} in all three cases. First hypothesis proposes an improvement of protective character of zinc areas due to formation of Mg^{2+}. Second hypothesis claims that presence of magnesium limits transfer of charge. Third hypothesis discusses about stabilisation of protective corrosion products such as simonkolleite ($Zn_5(OH)_8C_{l2}.H_2O$) and hydroxysulfate ($Zn_4(OH)_6SO_4.xH_2O$) by presence of Mg^{2+} which prevents their decomposition or transformation to less compact corrosion products [1].

Zn-Sn based alloys are characterized by good corrosion resistance and ductility [5]. Corrosion resistance of these alloys is not lower than of pure zinc but it depends on Zn-Sn ratio and corrosive environment. Tin is being used for various technological and economic reasons [6]. The motivation for tin addition into ternary Zn-Al-Mg was to characterize phase composition and corrosion behaviour as a function of Sn content. Possible variation in content of Zn_2Mg due to addition of Sn was predicted in literature [7]. Lower Zn_2Mg replaced by Mg_2Sn could provide beneficial mechanical properties, unless compromising corrosion properties significantly [8].

2. Experimental part

2.1. Sample preparation

Elements of 4N purity were melted in ceramic crucibles using furnace LAC LMV 5/12 at temperature of 480˚C. Homogenization of melt lasted approximately an hour and solidification of alloys was held outside the furnace on still air. Ingots were thereafter turned by lathe and cut into discs with dimensions ø30 x 8 mm. Chemical composition of ingots was verified using optical emission spectrometer Spectruma GDA 750. Table 1 shows results of this verification.

Samples were prepared by standard metallographic preparation including grinding using SiC papers from grit 240 to 4000, polishing from 3 µm to 0.25 µm using water free diamond slurries and etching with 0.3% Nital.

2.2. Microstructural analysis

Microstructural analysis of as-cast samples was executed using light microscope ZEISS Axiolmager.Z2m and scanning electron microscope JEOL JSM 7600F with FEG cathode. Back scattered electrons BSE collected with Retractable Backscattered Electrons Imaging (RBEI) detector were used to compose images of microstructure in z-contrast. Local chemical composition was determined using EDX detector Oxford Instruments X-Max 50 mm^2. Observations were performed using 15 kV accelerating voltage, 89 µA beam current and working distance was set to 15 mm.

Table 1.
Chemical composition of as-cast ingots in wt. %

Alloy	Zn	Al	Mg	Sn
Zn - 1.6 Al - 1.6 Mg	Bal.	1,87	1,58	–
Zn - 1.6 Al - 1.6 Mg - 0.5 Sn		1.97	1.94	0.51
Zn - 1.6 Al - 1.6 Mg - 1 Sn		2.01	1.98	1.05
Zn - 1.6 Al - 1.6 Mg - 2 Sn		1.98	2.21	2.71
Zn - 1.6 Al - 1.6 Mg - 3 Sn		2.03	2.08	2.98

2.3. XRD measurements

Phase composition of cast state was identified by XRD measurements. PANalytical Empyrean diffractometer with Bragg-Brentano geometry was used. Measurements were executed at room temperature and with sample spinning. The patterns were recorder over a two theta range 30-120° using iron filtered cobalt characteristic radiation. Powder samples made of ingots were used for more precise phase identification. For more accurate phase analysis of corroded surface a grazing incident GI XRD experiment was performed at constant ω angle (2°, 4° and 6°) at 2θ angle range from 5° up to 120°.

2.4. XRD measurements

In order to characterize complexity of phase transformations during solidification and cooling from molten state DSC experiments were suggested. After cutting thin pieces from an ingot, a small, max. 5 mg sample was prepared, weighted using precision laboratory balance Mettler Toledo and placed in graphite crucible. Melting temperature and temperatures of phase transformations were observed using power compensated differential scanning calorimeter Perkin Elmer Diamond DSC. Sample was heated up to 480 °C and cooled down with rate of 10°C/min with short equilibrating step at 480°C with dwell time of 10 minutes.

2.5. Corrosion test

Samples for corrosion test were painted by protective layer of Lacomit varnish on edges, sides and back. Only front polished face was exposed to a corrosive environment in corrosion chamber. Input information for corrosion test is sample weight before experiment and before painting and exposed surface area after painting. As corrosive environment in corrosion chamber CO.FO.ME.GRA 400LE a 5% water solution of analytical grade NaCl was used. Temperature in chamber was set to 35°C and exposure time was set to 250 h and 500 h. Cleaning of samples after exposure was performed using 10% water solution of CrO_3 assisted with ultrasonic cleaner. Cleaning procedure consisted of several consecutive steps. In each step a sample was immersed in CrO_3 and its weight was measured using laboratory scale Mettler Toledo XP204. This procedure was repeated till the weight changes levelled off and assumption was made that all corrosion products were removed.

3. Results

3.1. Microstructural analysis

SEM observation of microstructure has revealed a dendritic solidification microstructure typical for cast state. Fig.1 and Fig. 2 portrays solidification microstructures of two alloys where main phases are recognizable such as primary dendrites, monotectoid and binary and ternary eutectics. Chemical composition of individual phases was determined by EDX analysis. At least five distinct chemical compositions were recognized as it is shown in Tab. 3 corresponding to: Zn-rich solid solution; binary eutectic of Zn and Al rich solid solution; Zn and Mg rich phase with Zn/Mg ration 2/1; Zn and Sn rich phase with Zn/Sn ratio 2/1 and monotectoid consisting of Zn rich solid solution and Al rich solid solution.

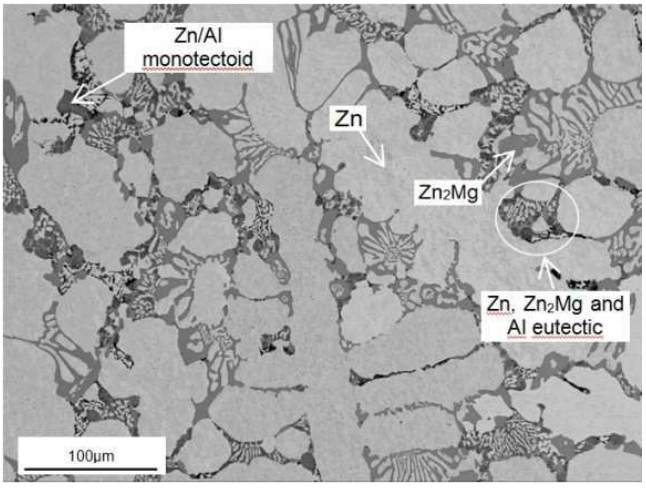

Fig.1 Microstructure of as-cast state of Zn-1.6Al-1.6Mg-0.5Sn

3.2. XRD measurements

For illustration purposes diffractograms of Zn-1.6Al-1.6Mg-0.5Sn and Zn-1.6Al-1.6Mg-3Sn are shown in Fig. 3. Alloys were found to contain solid solution of Zn, Zn_2Mg and Al solid solution. Alloy containing 3% of Sn contains also Mg_2Sn intermetallic phase. Table 2 shows results of quantitative phase analysis using the Rietveld method. Both, diffraction patterns as well as quantitative results confirm gradual decrease in quantity of $Zn_{11}Mg_2$ phase with increasing Sn content. Contrary, quantity of Mg_2Sn is increasing with Sn content. Quantity of Zn_2Mg reaches its maximum at 1 wt. % of Sn.

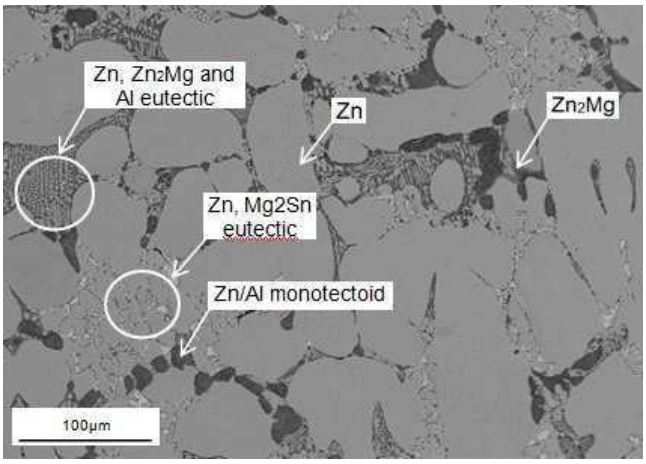

Fig. 2. Microstructure of as-cast state of Zn-1.6Al-1.6Mg-3Sn

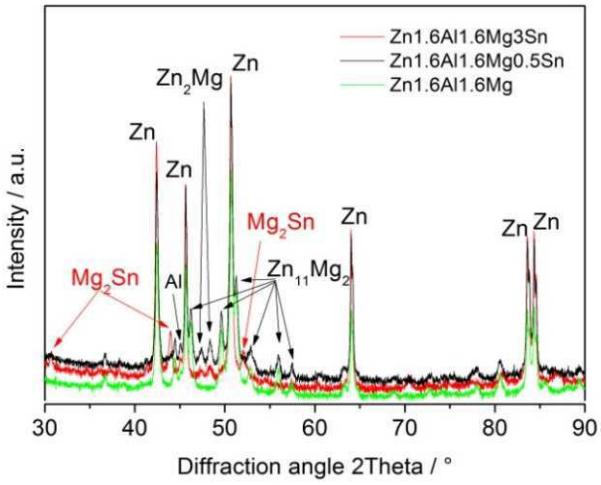

Fig. 3. Diffraction patterns of as-cast ingots of Zn-1.6Al-1.6Mg-0.5Sn and Zn-1.6Al-1.6Mg-3Sn

3.3. DSC experiment

As-cast microstructure evolves upon cooling during solidification. DSC experiment reveals that studied alloys transform from liquid into solid state in a series of transformations shown in Fig. 4. Reactions are recorded during DSC measurement as individual well resolved or overlapping exotherms. In case of all alloys, the beginning of solidification takes place by crystallizing Zn-reach solid solution at around 360°C which manifested by formation of Zn-based dendrites (see Fig. 1 and 2). Further crystallization events were observed at around 340°C and 330°C corresponding to a formation of other phases: Zn_2Mg, Mg_2Sn, Al solid solution along with Zn-based solid solution identified by SEM and XRD. In analogy with ternary Zn-Al-Mg it is assumed that Zn-based solid solution and Zn_2Mg forms binary eutectic shown in Fig. 1. Solidification process is terminated by ternary eutectic reaction involving Zn solid solution, Zn_2Mg and Al solid solution [8]. Exact sequence of reactions after Sn addition is subject of further analysis. XRD analysis together with microstructure evolution shown in Fig. 2 demonstrates formation of Mg_2Sn phase as a part of eutectic reaction.

Table 2.
Results of quantitative X-ray diffraction phase analysis

Alloy	Phase				
	Zn	Zn_2Mg	$Zn_{11}Mg_2$	Mg_2Sn	Al
Zn-1.6Al-1.6Mg	54.6 ±2.20	3.2 ±0.10	35.4 ±1.40	0	6.8 ±0.30
Zn-1.6Al-1.6Mg-0.5Sn	67.66 ±6.37	7.85 ±0.75	16.77 ±1.70	1.79 ±0.25	5.87 ±0.59
Zn-1.6Al-1.6Mg-1Sn	77.25 ±2.36	13.96 ±0.43	–	2.17 ±0.66	6.62 ±0.2
Zn-1.6Al-1.6Mg-2Sn	76.8 ±2.08	10.00 ±0.38	–	6.35 ±0.19	6.9 ±0.33
Zn-1.6Al-1.6Mg-3Sn	84.76 ±2.32	3.79 ±0.10	–	6.63 ±0.18	4.8 ±0.13

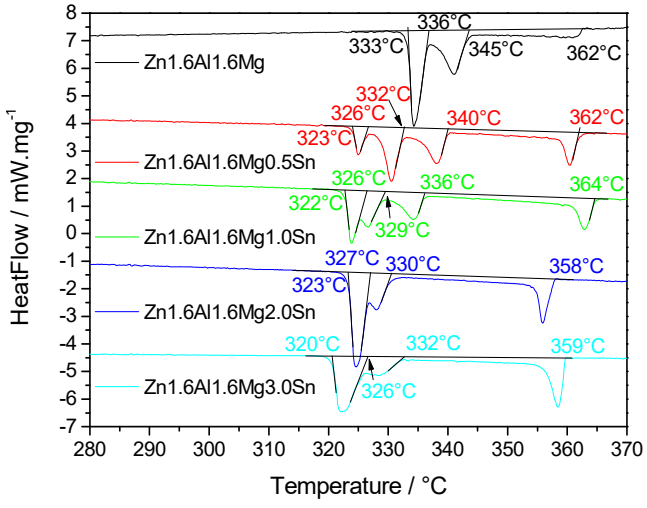

Fig. 4. As-cast microstructure of the Zn-Al-Mg-Sn ingots: a) Zn-1.6Al-1.6Mg b) Zn-1.6Al-1.6Mg-0.5Sn, c) Zn-1.6Al-1.6Mg-1.0Sn, d) Zn-1.6Al-1.6Mg-2.0Sn and e) Zn-1.6Al-1.6Mg-3.0Sn

3.4. Corrosion test

Samples were exposed to corrosive environment in a salt spray chamber for a period of 250 h and 500 h. Evolved corrosion products were analyzed using XRD in grazing incidence mode. Samples cleaned from corrosion products were subsequently measured for actual weight after the salt spray test (SST). Summary of results is shown in Table 3 and Table 4 and documents that samples of all experimental alloys containing Sn gained weight despite thorough surface cleaning.

In fact, sample after cleaning regained former luster of metallographic polishing as it is shown in Fig. 5 in case of Zn-1.6Al-1.6Mg-3Sn. Removal of corrosion products from the surface of this particular sample revealed formation of macroscopic blisters (Fig. 5).

Height of blisters was determined using laser scanning confocal microscope with profile analysis and reached approximately 40 μm, as it is shown in Fig. 6.

Table 3.
Sample weight after 250h of SST

Sample	Weight before SST [g]	Weight after SST [g]	Δ [g]
Zn-1.6Al-1.6Mg	33.6509	33.6447	-0.0063
Zn-1.6Al-1.6Mg-0.5Sn	40.8488	40.8525	+0.0037
Zn-1.6Al-1.6Mg-1Sn	31.6275	31.6307	+0.0032
Zn-1.6Al-1.6Mg-2Sn	33.2946	33.2995	+0.0049
Zn-1.6Al-1.6Mg-3Sn	32.2053	32.2352	+0.0299

Table 4.
Sample weight after 500h of SST

Sample	Weight before SST [g]	Weight after SST [g]	Δ (g)
Zn-1.6Al-1.6Mg	30.8675	30.8590	-0.0085
Zn-1.6Al-1.6Mg-0.5Sn	37.2626	37.2647	+0.0021
Zn-1.6Al-1.6Mg-1Sn	35.0866	35.0895	+0.0029
Zn-1.6Al-1.6Mg-2Sn	32.0795	32.0914	+0.0119
Zn-1.6Al-1.6Mg-3Sn	34.2982	34.3451	+0.0469

Due to observed unexpected change weight as well as visual change of the surface a metallographic inspection was devised to allow detailed analysis. Metallographic cross-section shown in Fig. 7 provides insight into the blister volume (a). Significant portion of the alloy just below the surface was found severally influenced by exposure in salt spray chamber and contain high amount of cracks where higher concentration of Cl and O was determined. Cracks developed in the region where eutectics are localized in interdendritic spaces (b).

Fig. 5. Macroscopic appearance of Zn-1.6Al-1.6Mg-3Sn after 500h salt spray test

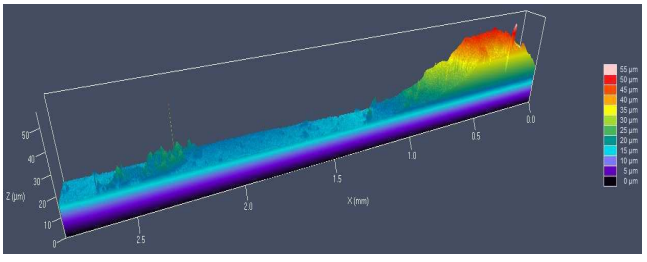

Fig. 6. Height profile evaluation of Zn-1.6Al-1.6Mg-3Sn after 500h of SST

According to GI XRD analysis of alloy Zn-1.6Al-1.6Mg-2Sn, corrosion products formed during SST consists of phases typical for as-cast state accompanied with simonkolleite, hydrotalcite after 250 hours (Fig. 8) and in addition also with hydrozincite after 500 hours of exposition (Fig. 9).

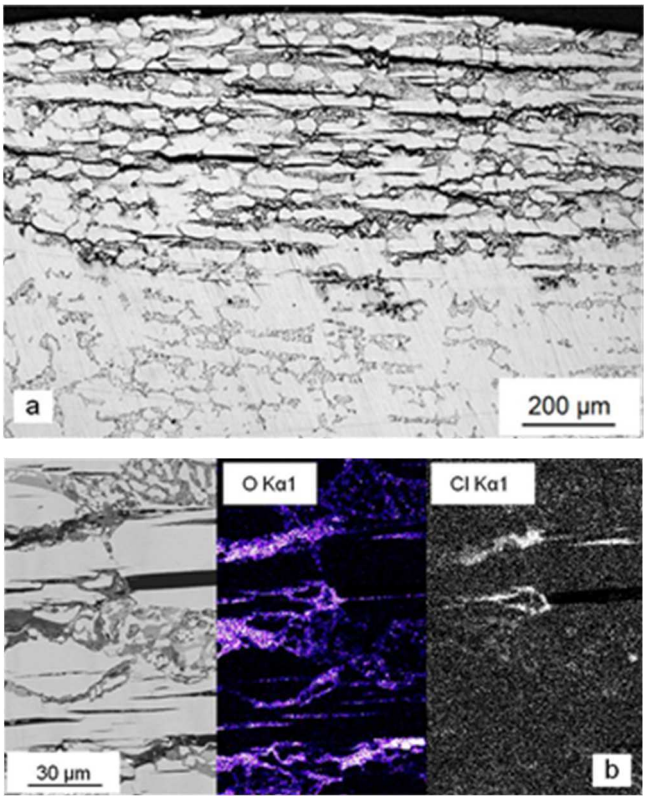

Fig. 7. Cross-section of a blister formed on the surface of an alloy containing Zn1.6Al1.6Mg3Sn. SEM z-contrast image (a) and corresponding O and Cl element map (b)

4. Conclusions

Ternary alloy Zn-1.6Al-1.6Mg was modified by addition of 0.5, 1, 2 and 3 wt% of Sn in order to observe a change in corrosion resistance in neutral salt spray chamber. Samples were prepared from ingots that solidified on air. Microstructure was observed using SEM and light microscopy. Phase composition was determined by XRD analysis. Phase analysis showed that microstructure includes Zn solid solution, Al solid solution and intermetallic phases Zn_2Mg or $Zn_{11}Mg_2$ and Mg_2Sn forming eutectics. Based on results, the increasing addition of Sn led to a formation of Mg_2Sn at the expense of $Zn_{11}Mg_2$ intermetallic phase.

Formation of Mg_2Sn is according to [9] more favourable with respect to future mechanical properties and ductility of alloys. Samples were exposed to Cl containing corrosive environment for 250 and 500 hours. XRD analyses of exposed samples proved formation of typical corrosion products such as simonkolleite, hydrotalcite after 250 hours and in addition also hydrozincite after 500 hours. Weight change measurements before and after SST did not show a typical weight loss. Instead, a gradual weight gain was observed as it is shown in Table 3 and Table 4. Weight gain was similar for 0.5 and 1 wt. % addition of Sn. Compared to these, the addition of 2 and 3 wt. % Sn caused significantly higher weight gain and formation of macroscopic blisters which negatively influences corrosion resistance of alloy. This finding corroborates with results of other authors [10].

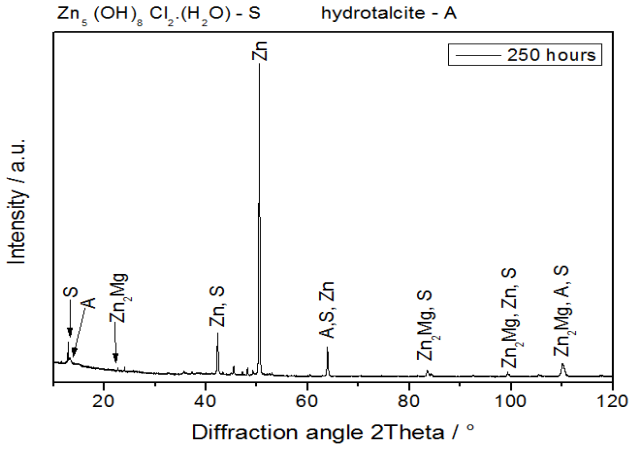

Fig. 8. GI XRD analysis of Zn1.6Al1.6Mg2.0Sn after salt spray test in a period of 250, where S holds for simonkolleite

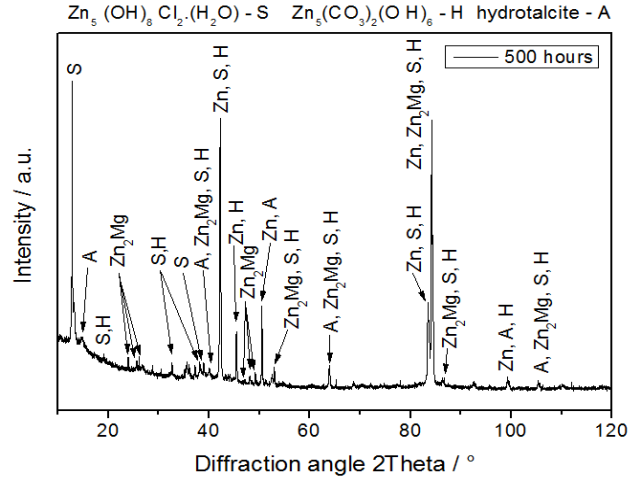

Fig. 9. GI XRD analysis of Zn1.6Al1.6Mg2.0Sn after salt spray test in a period of 500 hours, where S holds for simonkolleite and H for hydrozincite

Addition of tin had almost negligible effect on crystallisation onset of all studied alloys, which was found within interval of 6°C. However, tin influenced complexity of eutectic reactions. Ternary Zn-Al-Mg system solidified in

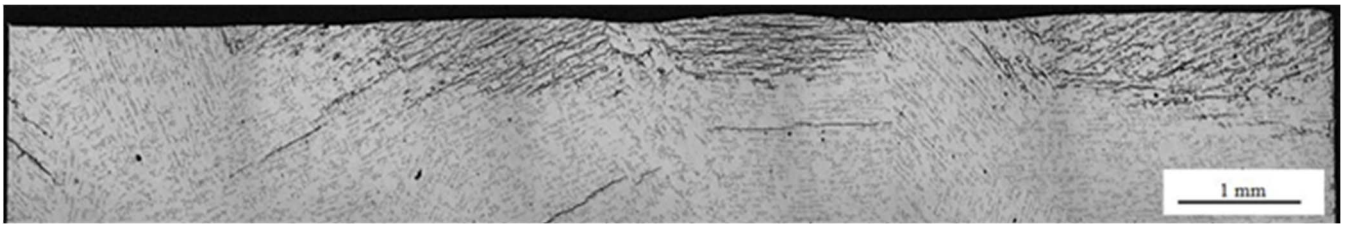

Fig. 10. View of dendrites orientation and their impact on surface corrosion resistance

two distinct reactions in the range from 345°C to 333°C. Addition of tin causes slight shift of eutectic reactions temperatures to lower values. Furthermore another apparent exothermic reaction is evolved in case of 0.5 and 1 wt.% Sn addition. It is assumed that this reaction is also present in case of 2 and 3 wt.% Sn addition but it is strongly overlapping with other reactions in this temperature region. The reaction overlapping causes that only two apparent exotherms are observed.

Metallographic cross-section of blisters was studied by light microscopy and SEM combined with oxygen and chlorine element mapping. Analysis of this area revealed extensive formation of corrosion products at the expense of phases located in interdendritic spaces, mainly eutectics and presence of oxides in cracks. These cracks were developed mainly in the direction of dendrite orientation (Fig.10), which has definite influence on corrosion resistance of surface. Dendrites growing in the direction parallel to the surface of the sample are strongly affected by corrosion propagation. If it was in perpendicular direction (90°), or in interval from 45 up 90° respectively, the surface remained almost unaffected. Such behavior suggests that formation of blisters is sensitive to crystallographic grain orientation with respect to exposed surface.

Acknowledgements

Authors would like to acknowledge financial support provided by Slovak Scientific Grant Agency VEGA in the frame of 1/0068/14 project.

Additional information

Selected issues related to this paper are planned to be presented at the 22nd Winter International Scientific Conference on Achievements in Mechanical and Materials Engineering Winter-AMME'2015 in the framework of the Bidisciplinary Occasional Scientific Session BOSS'2015 celebrating the 10th anniversary of the foundation of the Association of Computational Materials Science and Surface Engineering and the World Academy of Materials and Manufacturing Engineering and of the foundation of the Worldwide Journal of Achievements in Materials and Manufacturing Engineering.

References

[1] P. Volovitch, N.T. Vu, C. Allély, A. Aal Abdel, K. Ogle, Understanding corrosion via corrosion product characterization: II. Role of alloying elements in improving the corrosion resistance of Zn–Al–Mg coatings on steel, Corrosion Science 53 (2011) 2437-2445.

[2] E.C. Lee, C.Y. Nian, Y.S. Tarng, Design of materials processing technologies, Archives of Materials Science and Engineering 28 (2007) 48-56.

[3] S. Schruerz, M. Fleischlanderl, G. H. Luckeneder, K. Preis, T. Haunschmied, G. Mori, A.C. Kneissl, Corrosion behaviour of Zn–Al–Mg coated steel sheet in sodium chloride-containing environment, Corrosion Science 51 (2009) 2355-2363.

[4] A. M. Salgueiro, C. Allély, K. Ogle, P. Volovitch, Corrosion mechanisms of Zn (Mg, Al) coated steel in accelerated tests and natural exposure: 1. The role of electrolyte composition in the nature of corrosion products and relative corrosion rate, Corrosion Science 90 (2015) 472-481.

[5] A. M. Salgueiro, C. Allély, K. Ogle, P. Volovitch, Corrosion mechanisms of Zn (Mg, Al) coated steel: 2. The effect of Mg and Al alloying on the formation and properties of corrosion products in different electrolytes, Corrosion Science 90 (2015) 482-490.

[6] K. Kyoo Young, Y. Boo Young, An electrochemical study on Zn-Sn-alloy-coated steel sheets deposited by vacuum evaporation. Part I: Surface and Technology 64/2 (1994) 99-110.

[7] P. Ghosh, M. Mezbahul-Islam, M. Medraj, Critical assessment and thermodynamic modeling of Mg–Zn, Mg–Sn, Sn–Zn and Mg–Sn–Zn systems. CALPHAD: Computer Coupling of Phase Diagrams and Thermochemistry 36 (2012) 28-43.

[8] E. De Bruycker, Z. Zermout, C. B. De Cooman, Zn-Al-Mg Coatings: Thermodynamic Analysis and Microstructure Related Properties, Materials Science Forum 539-543 (2007) 1276-1281.

[9] L. Sziráky, A. Cziráky, Z. Vértesy, L. Kiss, V. Ivanova, G. Raichevski, S. Vitkova, T. Marinova. Zn and Zn-Sn alloy coatings with and without chromate layers. Part I: Corrosion resistance and structural analysis, Journal of Applied Electrochemistry 29 (1999) 927-937.

[10] Y. G. Kweon, C. Coddet, Behavior in Seawater of Zinc-Base Coatings on Aluminum Alloy 5086, Corrosion 48/2 (1992) 97-102.